HHS Public Access

Author manuscript

Obesity (Silver Spring). Author manuscript; available in PMC 2022 August 01.

Published in final edited form as:

Obesity (Silver Spring). 2021 August ; 29(8): 1328–1337. doi:10.1002/oby.23201.

Nucleus accumbens microstructure mediates the relationship between obesity and eating behavior in adults

Amjad Samara[1], **Zhaolong Li**[1,2], **Jerrel Rutlin**[1], **Cyrus A. Raji**[3,4], **Peng Sun**[3], **Sheng-Kwei Song**[3], **Tamara Hershey**[1,3,4], **Sarah A. Eisenstein**[1,3]

[1]Department of Psychiatry, Washington University School of Medicine, St. Louis, Missouri, USA

[2]Department of Psychological and Brain Sciences, Washington University School of Medicine, St. Louis, Missouri, USA

[3]Mallinckrodt Institute of Radiology, Washington University School of Medicine, St. Louis, Missouri, USA

[4]Department of Neurology, Washington University School of Medicine, St. Louis, Missouri, USA

Abstract

Objective: Basal ganglia regions are part of the brain's reward-processing networks and are implicated in the neurobiology of obesity and eating disorders. This study examines basal ganglia microstructural properties in adults with and without obesity.

Methods: Diffusion basis spectrum imaging (DBSI) images were analyzed to obtain putative imaging markers of neuroinflammation. Relationships between basal ganglia DBSI metrics and reward sensitivity and eating behaviors were also explored.

Results: A total of 46 participants (25 people with obesity; aged 20–40 years; 37 women) were included. Relative to the people in the normal-weight group, people with obesity had smaller caudate and larger nucleus accumbens (NAcc) volumes ($p < 0.05$) and lower DBSI fiber fraction (reflecting apparent axonal/dendrite density) in NAcc and putamen, higher DBSI nonrestricted fraction (reflecting tissue edema) in NAcc and caudate, and higher DBSI restricted fraction (reflecting tissue cellularity) in putamen ($p \leq 0.01$, all). Increased emotional and reward eating behaviors were related to lower NAcc axonal/dendrite density and greater tissue edema ($p \leq 0.002$). The relationships between emotional eating and adiposity measures were mediated by NAcc microstructure.

Conclusions: These findings provide evidence that microstructural alterations in basal ganglia relate to obesity and insights linking NAcc microstructure and eating behavior in adults.

Correspondence Sarah A. Eisenstein, Assistant Professor, Psychiatry Department, Washington University School of Medicine, St. Louis, MO 63110, USA. seisens@wustl.edu.

AUTHOR CONTRIBUTIONS

SAE, TH, PS, and SKS designed the study. AS, ZL, and JR analyzed the imaging data and performed statistical analysis, and AS, CAR, and SAE wrote the manuscript. All authors critically reviewed and edited the manuscript.

CONFLICT OF INTEREST

The authors declared no conflict of interest.

INTRODUCTION

Obesity results from an imbalance between energy consumption and expenditure regulated in part by the brain. Homeostatic and nonhomeostatic brain pathways interact and contribute to feeding and energy balance (1). Nonhomeostatic pathways, including cortico-limbic structures such as the prefrontal cortex and nucleus accumbens (NAcc), process external sensory cues as well as reward, cognitive, and emotional factors to promote or inhibit food intake (2). Basal ganglia regions (i.e., caudate, putamen, globus pallidus, and NAcc) are involved in regulating food intake and physical activity (3,4), and basal ganglia circuitry is implicated in obesity and eating disorders (5). Magnetic resonance (MR) neuroimaging studies of basal ganglia macrostructure in people with obesity have generally found smaller volumes relative to normal-weight people (6), although this has been somewhat inconsistent (6,7). The NAcc, located within the ventral striatum, has warranted particular attention because it plays a central role in reward processing, appetitive behavior, and reinforcement learning (8) and because it is implicated in obesity and food addiction (5,9,10,11). However, the mechanisms underlying the association between the basal ganglia (including the NAcc), obesity, and eating behaviors in humans remain unclear. A greater understanding of these relationships could provide potential targets for therapeutic interventions, including deep brain stimulation and noninvasive neuromodulation (12,13).

One potential mechanism has arisen from animal studies that have identified obesity-related neuroinflammation in several brain regions (14). However, in humans, assessment of this phenomenon *in vivo* via imaging remains technically challenging. Diffusion MR is a recent technique that models specific tissue properties based on water diffusion and allows for the study of basal ganglia and other gray matter tissue microstructure and cytoarchitecture in relation to adiposity (15,16). Greater BMI has been associated with lower mean water diffusivity in the right globus pallidus and right putamen (15), and NAcc cell density, as measured by diffusion MR-based imaging, has been associated with children's weight and has predicted future weight gain after 1 year of follow-up (16). These measures have been interpreted as indirect indicators of neuroinflammation. Despite these promising findings, the relationships between obesity, basal ganglia microstructure, and eating-related behavior have not been addressed.

Diffusion basis spectrum imaging (DBSI) is a newer diffusion MR-based model used to evaluate both axonal/dendrite integrity and neuroinflammation-related tissue changes (17). DBSI derives both a spectrum of isotropic diffusion reflecting biological processes related to neuroinflammation, such as cellularity (restricted intracellular diffusion) and edema (nonrestricted extracellular diffusion), and anisotropic diffusion reflecting axonal integrity and myelination. DBSI metrics have been rigorously validated through Monte Carlo simulations, tissue phantoms, and histopathological evaluation (17–20). Using DBSI, we recently performed a voxelwise, white matter tract-focused approach and showed that adults with obesity have greater neuroinflammation and lower axonal integrity in several white matter tracts compared with normal-weight adults, and we replicated our findings in an independent cohort (21). We also showed that DBSI metrics indicative of neuroinflammation in the hippocampus and amygdala correlate with poor cognitive performance in one cohort.

In this study, we evaluated basal ganglia microstructure in people with obesity and people with normal weight using DBSI. We examined obesity-associated differences in DBSI metrics in the basal ganglia regions related to apparent axonal/dendrite density (DBSI fiber fraction [DBSI-FF]), increased extracellular space/tissue edema (DBSI nonrestricted fraction [DBSI-NRF]), and neuroinflammation-related cellularity (DBSI restricted fraction [DBSI-RF]). We investigated the relationships between self-reported eating and reward behaviors, adiposity, and basal ganglia microstructure. We also conducted mediation analyses to examine possible mechanisms underlying significant correlations, with a particular emphasis on the NAcc. We hypothesized that obesity would relate to lower axonal/dendrite integrity and greater neuroinflammation in basal ganglia regions compared with normal-weight controls. We also hypothesized that basal ganglia microstructure and volume would relate to eating and reward sensitivity across people with normal weight and people with obesity.

METHODS

Participants

All study procedures were approved by the Washington University School of Medicine Human Research Protection Office and were carried out in accordance with the principles expressed in the Declaration of Helsinki. All participants gave written informed consent prior to participation. Obesity was defined as BMI ≥ 30 kg/m^2. Normal weight was defined as BMI ≤ 25 kg/m^2. Height and weight measurements were obtained by a nurse. Body fat percentage was assessed using dual-energy x-ray absorptiometry using the GE Lunar iDXA (GE Healthcare, Chalfont St Giles, UK) (22). Data from individuals included in this study have been reported in previous publications (21,23,24,25,26). Potential participants were screened by oral glucose tolerance test (OGTT), comprehensive medical evaluation, psychiatric interview (Structured Clinical Interview for *Diagnostic and Statistical Manual of Mental Disorders* [Fourth Edition]) (27), and the Binge Eating Scale (28). Participants were excluded for a self-reported history of diabetes or OGTT fasting or 2-hour plasma glucose levels indicative of diabetes according to American Diabetes Association guidelines (29), history of major neurological or psychiatric diagnosis, eating disorders (including binge eating disorder), head trauma, any current or recent dopaminergic drug use (e.g., stimulants, agonists, bupropion, neuroleptics, metoclopramide), tobacco use during the past month, current heavy alcohol use (male individuals > 2 drinks per day, female individuals > 1 drink per day), and illicit drug use.

Eating and reward sensitivity self-report questionnaires

During the day of the OGTT, participants completed questionnaires for a self-reported assessment of eating and reward sensitivity behaviors, including: 1) eating behavior related to emotion, including avoidance of negative affect; 2) eating behavior related to reward, including craving for palatable foods and inability to limit intake of palatable foods; 3) non-food reward behavior, including approach, sensitivity, motivation, and expectancy toward non-food reward stimuli; 4) sensitivity to punishment, including behavioral inhibition and expectancy toward aversive non-food stimuli.

For each of these four domains, a summed *z* score for which higher values reflect a greater endorsement of the behavior, as aforementioned, was calculated for each participant. The questionnaires and domain *z* score calculations have been described in detail elsewhere (23).

Participants also completed delayed and probabilistic monetary reward discounting (DRD, PRD) tasks as described in a previous publication (25). An individual's degree of reward discounting was determined by area under the curve (AUC) calculation. AUC values range between 0.0 and 1.0 such that lower DRD-AUC indicates a greater preference for immediate smaller monetary rewards over delayed larger monetary rewards, and lower PRD-AUC indicates a greater preference for guaranteed smaller monetary rewards over less certain larger monetary rewards.

MR acquisition and image processing

Brain MR imaging (MRI) scans were acquired on a Siemens Trio 3-T scanner with a 20-channel head coil (Siemens, Erlangen, Germany). High-resolution T1-weighted anatomical images were obtained using a three-dimensional magnetization-prepared rapid gradient-echo (MPRAGE) sequence (sagittal orientation, repetition time [TR] = 2,400 milliseconds, echo time [TE] = 3.16 milliseconds, inversion time = 1,000 millseconds, voxel resolution = 1 × 1 × 1 mm^3, frames = 176, flip angle = 8°, field-of-view = 256 × 256 mm). Two echo planar diffusion tensor imaging (DTI) sequences of similar phase-encoding direction were acquired with 27 volumes each (transverse orientation, 2 × 2 × 2 mm^3 voxels, TR = 12,300 milliseconds, TE = 108 milliseconds, flip angle = 90°, 25 directions, b values ranging from 0 to 1,400 s/mm^2, and two nondiffusion weighted images).

All preprocessing steps for anatomical and DTI images were completed with FMRIB Software Library (FSL; Analysis Group, FMRIB, Oxford, UK) (30). Structural images were processed with *fsl_anat* (https://fsl.fmrib.ox.ac.uk/fsl/fslwiki/fsl_anat; Analysis Group, FMRIB), which performs bias-field correction, registration to Montreal Neurological Institute (MNI) standard space, and subcortical structure segmentation. DTI preprocessing steps included removal of nonbrain tissue and motion- and eddy-current distortions correction.

DBSI brain maps were calculated using in-house software scripted in MATLAB (MathWorks, Natick, Massachusetts) (17,31). DBSI models both isotropic and anisotropic diffusion fractions and produces several brain maps that are proxy measures of tissue microstructure, i.e., anisotropic DBSI-FF (indicates apparent axonal/dendrite density), isotropic DBSI-NRF ($f(D)$, $D = 0.3 – 3.0\ \mu m^2/ms$; indicates extracellular water/tissue edema), and isotropic DBSI-RF ($f(D)$, $D \leq 0.3\ \mu m^2/ms$; indicates inflammation-related cellularity). Examples of average DBSI maps of the healthy brain in the normal-weight group are shown in Figure 1. All DBSI maps were registered to structural T1-weighted images. The initial registration step was performed using FSL *epi_reg* function (Analysis Group, FMRIB) and a nondiffusion weighted (b0) image because it provides the best intensity contrast between different tissue types. The resulting transformation matrix was then applied to other DBSI maps using the FSL *applyxfm* function (Analysis Group, FMRIB). For all individuals, average DBSI metrics in basal ganglia regions were extracted

using regions of interest (ROIs) from FSL subcortical structure segmentation and included in further statistical analyses as described in the following section.

Statistical analysis

We used Student *t* tests, Mann-Whitney *U* tests, or χ^2 tests to assess differences in demographic variables. Effect sizes were calculated using Cohen's *d*. Basal ganglia volumes were normalized for total intracranial volumes (ICV). Right and left basal ganglia volumes and ROI DBSI metrics were averaged. Average behavioral domain summed *z* scores, basal ganglia volumes, and ROI DBSI metrics were compared between people with obesity and people with normal weight using a multiple linear regression model with age, sex, race, and level of education as covariates. We used partial Pearson *r* correlations, controlling for age, sex, race, and level of education, to relate basal ganglia volumes and ROI DBSI metrics to behavioral domain *z* scores. Basal ganglia DBSI metrics and behavioral domain *z* score correlations were Bonferroni-corrected for multiple comparisons ($\alpha = 0.05/[6$ behavioral domains × 4 brain regions] = 0.002). For significant correlations between ROI DBSI metrics and behavioral domain *z* scores, we conducted an exploratory mediation analysis to evaluate whether one or more mediators "M" (basal ganglia DBSI metric) mediate the relationship between an independent variable "X" (behavioral domain *z* score) and the dependent variable "Y" (adiposity measure). We used body fat percentage and BMI as adiposity measures in separate mediation analyses. Average causal mediation effects (indirect effect), average direct effects, proportions mediated, and total effect were computed. Mediation analyses were performed using nonparametric bootstrapping for confidence interval estimation with 1,000 Monte Carlo iterations with statistical significance at a threshold of corrected $p \leq 0.05$. Statistical analyses used R (version 3.6.3; R Foundation for Statistical Computing, Vienna, Austria) and its "mediation" statistical package.

RESULTS

Participant characteristics

Participant demographics, obesity-related measures, and behavioral scores are described in Table 1. A total of 25 people with obesity and 21 people with normal weight were included in the study (age range = 20–40 years). People with obesity were older, had a greater proportion of non-White individuals, and had fewer years of education than people with normal weight. The two groups did not differ significantly in sex distribution. For analyses involving DRD and PRD, data were missing for four participants (three people with obesity and one person with normal weight). Compared with those in the normal-weight group, people with obesity demonstrated significantly greater self-reported emotional eating, reward-related eating, and behavioral inhibition (sensitivity to punishment) and less self-reported non-food reward behavior. The two groups did not differ significantly in DRD-AUC or PRD-AUC. These comparisons and results are similar but slightly different from previous publications (23,25) because of variability in included participants (Table 1).

Basal ganglia volumetric and microstructural comparisons

People with obesity had significantly smaller ICV-corrected caudate volumes ($p = 0.0057$; Cohen's $d = 0.79$) and larger NAcc volumes ($p = 0.048$; Cohen's $d = 0.14$) than people

with normal weight. People with obesity also had smaller ICV-corrected putamen and globus pallidum volumes than people with normal weight, but these differences were not statistically significant ($p = 0.22$ and $p = 0.058$, respectively).

People with obesity had lower DBSI-FF in the NAcc ($p < 0.0001$; Cohen's $d = 1.33$) and putamen ($p = 0.0005$; Cohen's $d = 1.16$), higher DBSI-NRF in the NAcc ($p < 0.0001$; Cohen's $d = 0.97$) and caudate ($p = 0.01$; Cohen's $d = 0.71$), and higher DBSI-RF in the putamen ($p = 0.004$; Cohen's $d = 1.12$; Figure 2). No other DBSI metrics in the basal ganglia structures were significantly different between the two groups ($p \geq 0.05$). Means and standard deviations (SD) for volumes (mm^3) and DBSI metrics are listed in Table 2.

Relationships between eating/reward sensitivity summed *z* scores and basal ganglia microstructure

Greater emotional and reward-related eating summed *z* scores correlated with lower NAcc DBSI-FF and greater NAcc DBSI-NRF (Figure 3, left and middle panels). These correlations survived multiple comparison correction ($p = 0.002$, corrected). Emotional and reward-related eating summed *z* scores did not relate to NAcc volumes ($p = 0.21$ and $p = 0.2$, respectively). Greater DRD-AUC (meaning lower delayed monetary reward discounting; preference for delayed larger over immediate smaller rewards) related to greater caudate DBSI-FF but did not survive multiple comparison correction (Figure 3, right panel). DRD-AUC did not relate to caudate volume ($p = 0.66$). Putamen and globus pallidum volumes and DBSI metrics did not relate to self-reported behavior, DRD-AUC, or PRD-AUC ($p > 0.05$).

Mediation analyses found that DBSI-FF in the NAcc partially mediated the association between self-reported emotion-related eating and body fat percentage (Figure 4) and BMI (data not shown). Although greater emotion-related eating related to higher body fat percentage ($\beta = 1.2$; $p = 0.01$) and higher BMI ($\beta = 1.6$; $p < 0.01$), these relationships were weakened and they became nonsignificant after controlling for DBSI-FF in the NAcc as the mediator ($\beta = 0.74$, $p = 0.12$ for body fat percentage; $\beta = 0.72$, $p = 0.13$ for BMI). The proportions of the total effect mediated by NAcc DBSI-FF were estimated at 44% for body fat percentage ($p = 0.028$) and 56% for BMI ($p < 0.01$). The mediation analyses for the relationship between reward-related eating and body fat percentage or BMI, with NAcc DBSI metrics as mediators, were not significant (data not shown).

DISCUSSION

The results of our study show that obesity in adults is associated with alterations in basal ganglia volumes and tissue microstructure. Similar to some prior studies, people with obesity had lower caudate and higher NAcc volumes than people with normal weight. In addition, we report the novel finding that people with obesity have lower axonal/dendrite density in NAcc and putamen, greater tissue edema in caudate and NAcc, and greater neuroinflammation-related cellularity in the putamen relative to people with normal weight. Furthermore, NAcc microstructure mediated the relationship between self-reported emotion-related eating and adiposity measures (body fat percentage and BMI) across people with normal weight and people with obesity. To our knowledge, this is the first *in vivo* neuroimaging study to link NAcc microstructure to eating behavior in people with obesity

and people with normal weight. Interestingly, we did not observe these relationships with NAcc volume, suggesting that DBSI-measured microstructural properties could provide additional information over macrostructural measures.

Basal ganglia volume and microstructural changes related to obesity

In our analyses, people with obesity showed variably smaller volumes in caudate, putamen, and globus pallidus and larger volumes in the NAcc, similar to prior studies (6,32,33). Results from a meta-analysis have suggested that higher NAcc volume at a young age could be a vulnerability factor for obesity, whereas decreased NAcc volume with increased BMI in older adults is due to the prolonged influence of neuroinflammation on the brain (7). It is unknown whether these structural differences are a vulnerability factor for the development of obesity or a consequence of obesity-related neuroinflammation or other neurological alterations.

Microstructural evaluations of the basal ganglia could provide valuable insights into underlying changes in tissue that could be missed in volumetric studies. For example, using traditional DTI analyses, one study found increased mean diffusivity in the right putamen and right globus pallidus related to high BMI (15). However, multicompartment diffusion MRI models such as DBSI are capable of providing more accurate data about specific tissue microstructural changes than traditional DTI (21,34). Using restriction spectrum imaging (RSI), Rapuano et al. showed that NAcc cellular density (i.e., restricted isotropic component fraction) is higher in children with obesity, and NAcc microstructure is a significant predictor of weight gain after 1 year (16). The authors suggested that this finding could be related to increased glial cells (e.g., astrocytes, microglia), which is suggestive of local neuroinflammation. Using DBSI, we revealed similar NAcc microstructural changes in adults with obesity (i.e., lower apparent axonal/dendrite density and higher tissue edema/extracellular water diffusion). This pattern of changes in DBSI metrics is highly suggestive of neuroinflammation (17,19). Importantly, RSI applies a different theoretical model for diffusion imaging from DBSI (35). Unlike DBSI, RSI does not derive isotropic diffusion spectrum based on isotropic apparent diffusion coefficient. Instead, it assesses cellular density and structural signatures based on the ratio of axial and transverse diffusivities (35). Therefore, the exact interpretation or comparison of these surrogate diffusion-imaging markers would require additional studies employing both methods for a head-to-head comparison. Taken together, converging evidence from both DBSI and RSI studies support the notion that NAcc microstructural properties differ in children and adults with and without obesity.

Although it is plausible to hypothesize that NAcc microstructural changes are related to neuroinflammation, our DBSI findings should be interpreted with caution. Histological studies have indicated the great morphological complexity of the NAcc with several types of neurons exhibiting various soma size, morphology, dendrite/axonal patterns, and spine density (36). Moreover, the cellular density in the two NAcc subdivisions (core and shell) are normally variable, and each contains different predominant neuronal types (36). For example, a disproportionate increase or decrease in the volume of one NAcc subdivision might lead to marked overall differences in cellular density/microstructure in the absence

of a significant neuroinflammatory process. Therefore, future studies should combine MR-based and complementary neuroimaging methods such as positron emission tomography (PET) with a tracer that detects neuroinflammation to better understand the underlying cellular mechanism of altered NAcc microstructure.

Relationship between NAcc microstructure and eating behavior

Unhealthy eating habits, such as emotional and reward-related eating, contribute to overeating and increase the risk for obesity (37,38). In our study, people with obesity demonstrated significantly greater self-reported eating related to both emotion and reward compared with people in the normal-weight group. In a previous study, we showed that greater self-reported emotional eating relates to greater striatal D2 dopamine receptor binding across people with normal weight and people with obesity using PET imaging (23). Identifying additional structural and functional brain correlates of emotional and reward-related eating derived from MRI could provide helpful insights for the prevention and treatment of obesity and appetitive disorders. A substantial body of evidence demonstrates that the NAcc is implicated in the promotion of unhealthy eating habits, food addiction, and reward-motivated behaviors (5,39). For example, Abdo et al. studied 466 participants with and without binge eating disorder and showed a positive correlation between left NAcc volume and binge-eating score (40). Our findings establish a strong relationship between NAcc microstructure and eating behavior. Notably, our correlation and mediation findings were specific to the NAcc and were not detected in other basal ganglia regions involved in reward processing, although our small sample size may have limited our power to detect smaller effects. Therefore, the current findings should be confirmed by replication in future, larger studies. The specific mechanism linking NAcc microstructure to emotional and reward-related eating is still unknown. Neuroinflammation is one potential mechanism. With animal models of obesity, a high-fat diet triggers pro-inflammatory signs in the NAcc, such as reactive gliosis and increased expression of pro-inflammatory cytokines (41). The NAcc inflammation process, in turn, contributes to eating behavior changes characterized by compulsive sucrose seeking (41). Interestingly, it is also possible that neuroinflammation in the NAcc could disrupt dopaminergic neurotransmission, leading to deficits in reward processing in a manner that increases appetite and food intake (42).

Limitations and directions for future research

Our study's main limitation is the modest sample size, and that the majority of the included participants were women, which restricted our ability to investigate sex-related effects. The link between obesity and gray matter volumes in reward-associated regions has been reported to be stronger in women (43,44). Second, behavior that is self-reported via questionnaires is subjective and prone to recall error and/or demand characteristics. In future studies, behavior should also be evaluated using activities for which blinded and automated scoring is possible. Third, we used the traditional interpretations of DBSI metrics to infer NAcc tissue microstructural properties (i.e., DBSI-FF, as a proxy measure of axonal/dendrite density and DBSI-NRF as a proxy measure of neuroinflammation-related edema). However, DBSI has not been histopathologically validated for basal ganglia gray matter microstructure and pathology. Therefore, we could not draw definitive conclusions about the underlying mechanism responsible for the basal ganglia tissue changes related to

obesity. Future studies should include longitudinal follow-ups and collect complementary neuroinflammation measures such as PET radiotracer and plasma or cerebrospinal fluid inflammatory marker levels.

CONCLUSION

In conclusion, our study provides evidence that obesity is associated with significant microstructural alterations in basal ganglia regions, particularly the NAcc. We showed that these alterations are suggestive of neuroinflammation and that they could be linked to eating and reward-related behavior, contributing to overeating and obesity. Future longitudinal studies should include larger sample sizes and explore the temporal relationships between eating behavior, brain microstructure, and obesity. Such studies could then reveal whether these structural differences are a risk factor for the development of obesity and/or a consequence of obesity-related neuroinflammation.

FUNDING AGENCIES

This work was supported by the National Institutes of Health (NIH) (R01 DK085575, T32 DA007261–29), Washington University in St. Louis NIH KL2 Grant (KL2 TR000450 – ICTS Multidisciplinary Clinical Research Career Development Program), the Radiological Society of North America Research Scholar Grant, and the Clinical and Translational Science Award (UL1 TR000448). The funders had no role in study design, data collection, and analysis, decision to publish, or preparation of the manuscript.

Funding information

National Institute on Drug Abuse, Grant/Award Number: T32 DA007261–29; National Institutes of Health, Grant/Award Number: KL2 TR000450 and R01 DK085575

REFERENCES

1. Berthoud HR. Homeostatic and non-homeostatic pathways involved in the control of food intake and energy balance. Obesity (Silver Spring). 2006;14(suppl 5):197s–200s. [PubMed: 17021366]
2. Cardinal RN, Parkinson JA, Hall J, Everitt BJ. Emotion and motivation: the role of the amygdala, ventral striatum, and prefrontal cortex. Neurosci Biobehav Rev. 2002;26(3):321–352. [PubMed: 12034134]
3. Friend DM, Devarakonda K, O'Neal TJ, et al. Basal ganglia dysfunction contributes to physical inactivity in obesity. Cell Metab. 2017;25(2):312–321. [PubMed: 28041956]
4. Wang G-J, Volkow ND, Logan J, et al. Brain dopamine and obesity. Lancet. 2001;357(9253):354–357. [PubMed: 11210998]
5. Volkow ND, Wang GJ, Tomasi D, Baler RD. Obesity and addiction: neurobiological overlaps. Obes Rev. 2013;14(1):2–18. [PubMed: 23016694]
6. Dekkers IA, Jansen PR, Lamb HJ. Obesity, brain volume, and white matter microstructure at MRI: a cross-sectional UK Biobank study. Radiology. 2019;291(3):763–771. [PubMed: 31012815]
7. García-García IF, Morys F, Dagher A. Nucleus accumbens volume is related to obesity measures in an age-dependent fashion. J Neuroendocrinol. 2019;e12812. doi:10.1111/jne.12812 [PubMed: 31758711]
8. Maldonado-Irizarry CS, Swanson CJ, Kelley AE. Glutamate receptors in the nucleus accumbens shell control feeding behavior via the lateral hypothalamus. J Neurosci. 1995;15(10):6779–6788. [PubMed: 7472436]
9. Domingo-Rodriguez L, Ruiz de Azua I, Dominguez E, et al. A specific prelimbic-nucleus accumbens pathway controls resilience versus vulnerability to food addiction. Nat Commun. 2020;11(1):782. doi:10.1038/s41467-020-14458-y [PubMed: 32034128]

10. Peciña S, Berridge KC. Hedonic hot spot in nucleus accumbens shell: where do mu-opioids cause increased hedonic impact of sweetness? J Neurosci. 2005;25(50):11777–11786. [PubMed: 16354936]
11. Robinson MJF, Burghardt PR, Patterson CM, et al. Individual differences in cue-induced motivation and striatal systems in rats susceptible to diet-induced obesity. Neuropsychopharmacology. 2015;40(9):2113–2123. [PubMed: 25761571]
12. Formolo DA, Gaspar JM, Melo HM, et al. Deep brain stimulation for obesity: a review and future directions. Front Neurosci. 2019;13:323. doi:10.3389/fnins.2019.00323 [PubMed: 31057350]
13. Whiting AC, Oh MY, Whiting DM. Deep brain stimulation for appetite disorders: a review. Neurosurg Focus. 2018;45(2):E9. doi:10.3171/2018.4.FOCUS18141
14. Guillemot-Legris O, Muccioli GG. Obesity-induced neuroinflammation: beyond the hypothalamus. Trends Neurosci. 2017;40(4):237–253. [PubMed: 28318543]
15. Takeuchi H, Taki Y, Nouchi R, et al. The associations of BMI with mean diffusivity of basal ganglia among young adults with mild obesity and without obesity. Sci Rep. 2020;10(1):12566. doi:10.1038/s41598-020-69438-5 [PubMed: 32724120]
16. Rapuano KM, Laurent JS, Hagler DJ, et al. Nucleus accumbens cytoarchitecture predicts weight gain in children. Proc Natl Acad Sci U S A. 2020;117(43):26977–26984. [PubMed: 33046629]
17. Wang Y, Wang Q, Haldar JP, et al. Quantification of increased cellularity during inflammatory demyelination. Brain. 2011;134(pt 12):3590–3601. [PubMed: 22171354]
18. Wang X, Cusick MF, Wang Y, et al. Diffusion basis spectrum imaging detects and distinguishes coexisting subclinical inflammation, demyelination and axonal injury in experimental autoimmune encephalomyelitis mice. NMR Biomed. 2014;27(7):843–852. [PubMed: 24816651]
19. Wang Y, Sun P, Wang Q, et al. Differentiation and quantification of inflammation, demyelination and axon injury or loss in multiple sclerosis. Brain. 2015;138(pt 5):1223–1238. [PubMed: 25724201]
20. Chiang C-W, Wang Y, Sun P, et al. Quantifying white matter tract diffusion parameters in the presence of increased extra-fiber cellularity and vasogenic edema. NeuroImage. 2014;101:310–319. [PubMed: 25017446]
21. Samara A, Murphy T, Strain J, et al. Neuroinflammation and white matter alterations in obesity assessed by diffusion basis spectrum imaging. Front Hum Neurosci. 2019;13:464. doi:10.3389/fnhum.2019.00464 [PubMed: 31992978]
22. Hind K, Oldroyd B, Truscott JG. In vivo precision of the GE Lunar iDXA densitometer for the measurement of total body composition and fat distribution in adults. Eur J Clin Nutr. 2011;65(1):140–142. [PubMed: 20842171]
23. Eisenstein SA, Bischoff AN, Gredysa DM, et al. Emotional eating phenotype is associated with central dopamine D2 receptor binding independent of body mass index. Sci Rep. 2015;5:11283. doi:10.1038/srep11283 [PubMed: 26066863]
24. Eisenstein SA, Antenor-Dorsey JA, Gredysa DM, et al. A comparison of D2 receptor specific binding in obese and normal-weight individuals using PET with (N-[(11)C]methyl)benperidol. Synapse. 2013;67(11):748–756. [PubMed: 23650017]
25. Eisenstein SA, Gredysa DM, Antenor–Dorsey JA, et al. Insulin, central dopamine D2 receptors, and monetary reward discounting in obesity. PLoS One. 2015;10(7):e0133621. doi:10.1371/journal.pone.0133621 [PubMed: 26192187]
26. Eisenstein SA, Koller JM, Piccirillo M, et al. Characterization of extrastriatal D2 in vivo specific binding of [^{18}F](N-methyl)benperidol using PET. Synapse. 2012;66(9):770–780. [PubMed: 22535514]
27. First MB, Spitzer RL, Gibbon M, Williams JBW. Structured Clinical Interview for DSM-IV-TR Axis I Disorders, Research Version, Patient Edition with Psychotic Screen (SCID-I/P W/PSY SCREEN). New York, NY: New York State Psychiatric Institute; 2002.
28. Gormally J, Black S, Daston S, Rardin D. The assessment of binge eating severity among obese persons. Addict Behav. 1982;7(1):47–55. [PubMed: 7080884]
29. American Diabetes Association. Standards of medical care in diabetes–2010. Diabetes Care. 2010;33(suppl 1):S11–S61. [PubMed: 20042772]

30. Smith SM, Jenkinson M, Woolrich MW, et al. Advances in functional and structural MR image analysis and implementation as FSL. NeuroImage. 2004;23(suppl 1):S208–S219. [PubMed: 15501092]

31. Chow N, Hwang KS, Hurtz S, et al. Comparing 3T and 1.5T MRI for mapping hippocampal atrophy in the Alzheimer's Disease Neuroimaging Initiative. AJNR Am J Neuroradiol. 2015;36(4):653–660. [PubMed: 25614473]

32. Janowitz D, Wittfeld K, Terock J, et al. Association between waist circumference and gray matter volume in 2344 individuals from two adult community-based samples. NeuroImage. 2015;122:149–157. [PubMed: 26256530]

33. Pannacciulli N, Del Parigi A, Chen K, Le DS, Reiman EM, Tataranni PA. Brain abnormalities in human obesity: a voxel-based morphometric study. NeuroImage. 2006;31(4):1419–1425. [PubMed: 16545583]

34. Cross AH, Song SK. A new imaging modality to non-invasively assess multiple sclerosis pathology. J Neuroimmunol. 2017;304:81–85. [PubMed: 27773433]

35. White NS, Leergaard TB, D'Arceuil H, Bjaalie JG, Dale AM. Probing tissue microstructure with restriction spectrum imaging: Histological and theoretical validation. Hum Brain Mapp. 2013;34(2):327–346. [PubMed: 23169482]

36. Sazdanovic M, Sazdanovic P, Zivanovic-Macuzic I, et al. Neurons of human nucleus accumbens. Vojnosanit Pregl. 2011;68(8):655–660. [PubMed: 21991788]

37. Gibson EL. Emotional influences on food choice: sensory, physiological and psychological pathways. Physiol Behav. 2006;89:53–61. [PubMed: 16545403]

38. Dallman MF. Stress-induced obesity and the emotional nervous system. Trends Endocrinol Metab. 2010;21(3):159–165. [PubMed: 19926299]

39. Berthoud HR, Morrison C. The brain, appetite, and obesity. Annu Rev Psychol. 2008;59:55–92. [PubMed: 18154499]

40. Abdo N, Boyd E, Baboumian S, Pantazatos SP, Geliebter A. Relationship between binge eating and associated eating behaviors with subcortical brain volumes and cortical thickness. J Affect Disord. 2020;274:1201–1205. [PubMed: 32663951]

41. Décarie-Spain L, Sharma S, Hryhorczuk C, et al. Nucleus accumbens inflammation mediates anxiodepressive behavior and compulsive sucrose seeking elicited by saturated dietary fat. Mol Metab. 2018;10:1–13. [PubMed: 29454579]

42. Leite F, Ribeiro L. Dopaminergic pathways in obesity-associated inflammation. J Neuroimmune Pharmacol. 2020;15(1):93–113. [PubMed: 31317376]

43. Horstmann A, Busse FP, Mathar D, et al. Obesity-related differences between women and men in brain structure and goal-directed behavior. Front Hum Neurosci. 2011;5:58.doi:10.3389/fnhum.2011.00058 [PubMed: 21713067]

44. Kroll DS, Feldman DE, Biesecker CL et al. Neuroimaging of sex/gender differences in obesity: a review of structure, function, and neurotransmission. Nutrients. 2020;12(7):1942. doi:10.3390/nu12071942

Study Importance

What is already known?

- Basal ganglia regions (i.e., caudate, putamen, globus pallidus, and nucleus accumbens [NAcc]) are involved in regulating food intake and have been implicated in obesity and eating disorders.
- Magnetic resonance neuroimaging studies of basal ganglia macrostructure in people with obesity generally find smaller volumes relative to normal-weight people, although these findings are somewhat inconsistent.

What does this study add?

- Obesity is associated with significant microstructural alterations in basal ganglia regions, particularly the NAcc.
- The observed basal ganglia microstructural alterations, assessed with diffusion basis spectrum imaging, are suggestive of neuroinflammation.
- NAcc microstructure relates to emotional and reward-related eating, and NAcc axonal density mediates the relationship between emotional eating and adiposity measures.

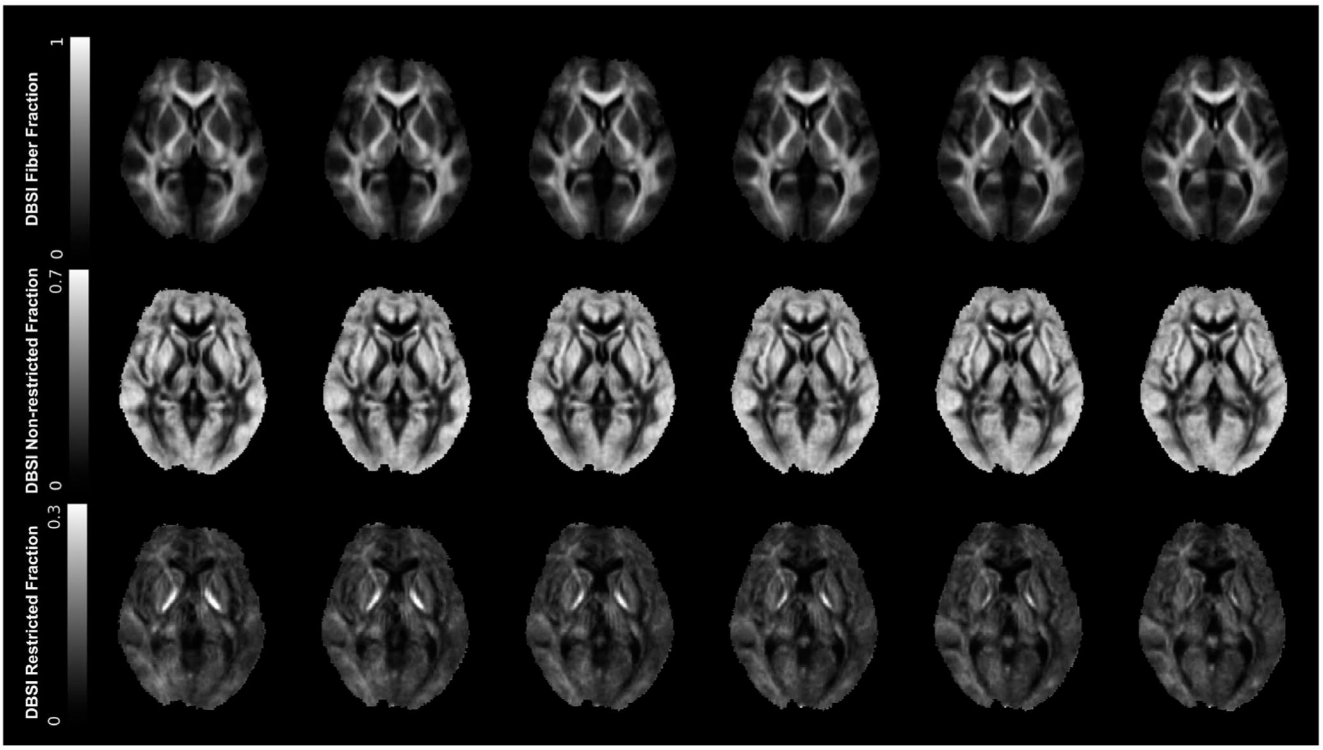

FIGURE 1.

Average DBSI from the normal-weight group ($n = 21$). DBSI fiber fraction (top row) is an indicator of anisotropic water diffusion or apparent axonal/dendrite density, and it shows the highest intensity in white matter tracts. DBSI nonrestricted fraction (middle row) is an indicator of isotropic extracellular water diffusion or tissue edema. DBSI restricted fraction (bottom row) is an indicator of intracellular isotropic restricted diffusion or increased tissue cellularity. DBSI, diffusion basis spectrum imaging

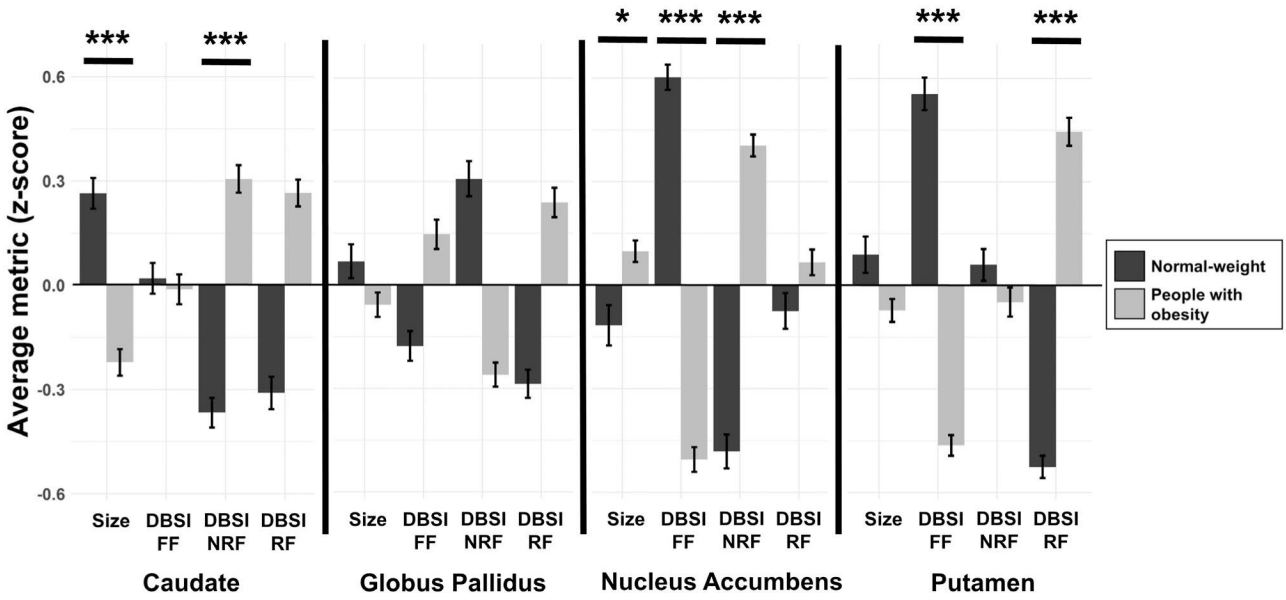

FIGURE 2.

Comparison of basal ganglia volumes and microstructure between people with obesity and people with normal weight. Volumes are corrected for total intracranial volumes. For scaling, average volume and DBSI metrics in regions of interest were converted to *z* scores. Error bars, mean ± SE. *$p \leq 0.05$ and *** $p \leq 0.01$ relative to normal-weight group. DBSI, diffusion basis spectrum imaging; FF, fiber fraction; NRF, nonrestricted fraction; RF, restricted fraction

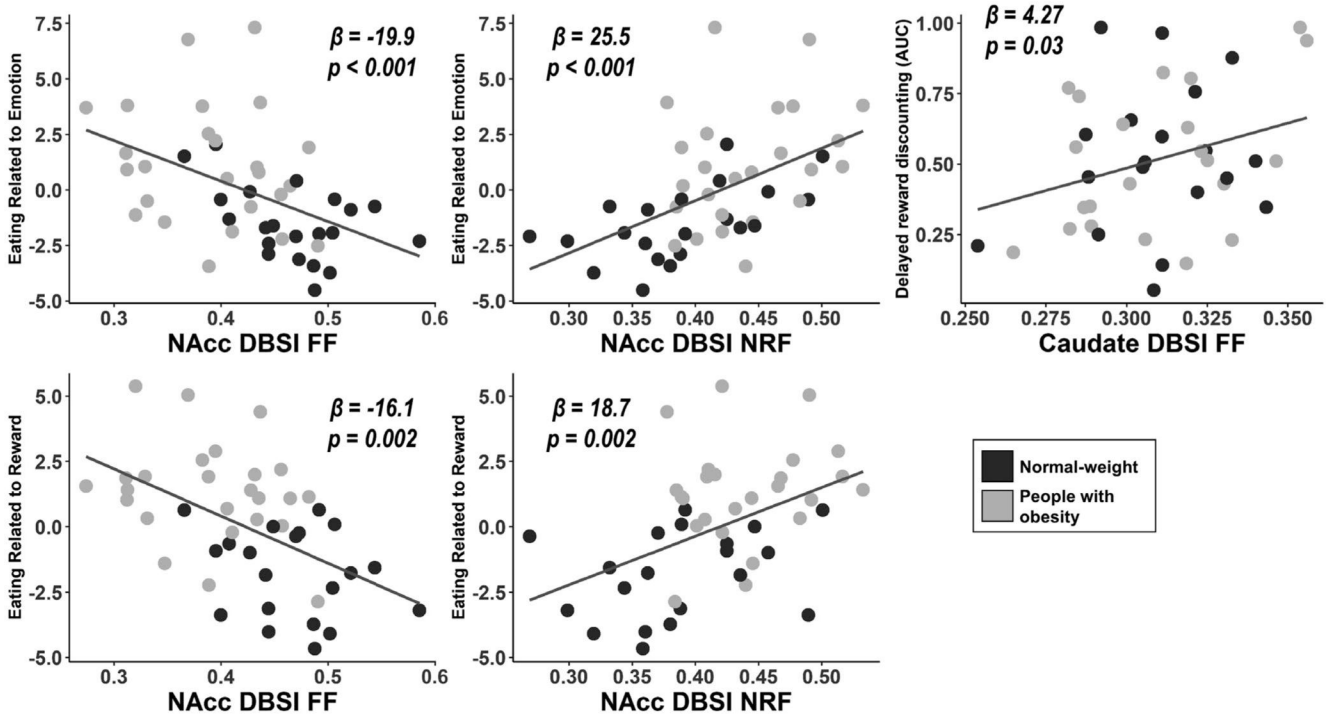

FIGURE 3.

Significant correlations between eating and reward-related behavior and average DBSI metrics in basal ganglia structures, controlling for age, sex, race, and level of education. Greater eating related to emotion and eating related to reward behaviors related to lower DBSI-FF and greater DBSI-NRF in NAcc. Higher DRD-AUC (lower delayed monetary reward discounting) related to greater caudate DBSI-FF. AUC, area under the curve; DBSI, diffusion basis spectrum imaging; DRD, delayed reward discounting; FF, fiber fraction; NAcc, nucleus accumbens; NRF, nonrestricted fraction

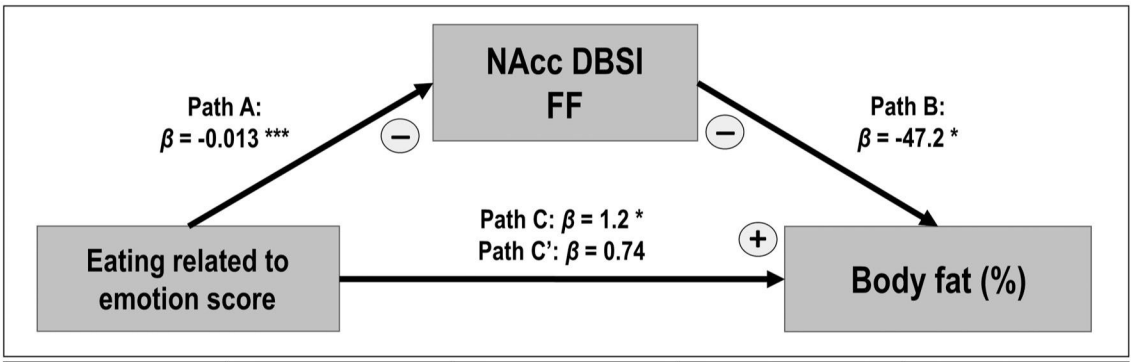

	Estimate	95% CI Lower	95% CI Upper	*p*-value
ACME	0.59	0.07	1.29	0.026 *
ADE	0.74	-0.14	1.93	0.114
Total Effect	1.33	0.59	2.42	< 0.001 ***
Prop. Mediated	0.44	0.04	1.17	0.028 *

FIGURE 4.

Mediation analysis represented as a path model diagram. The model shows the relationship between self-reported emotional eating and body fat percentage as mediated by NAcc DBSI-FF across people with normal weight and people with obesity. The total β effect (Path C) represents the effect of the independent variable without mediators (statistically significant). Direct β effect (Path C') represents the effect of the independent variable with NAcc DBSI-FF included in the model as a mediator (statistically nonsignificant). The indirect effects (Path A-B) represent the effect of the independent variable through the mediator (statistically significant). *$p \leq 0.05$ and ***$p \leq 0.01$. ACME, average causal mediation effects; ADE, average direct effects; DBSI, diffusion basis spectrum imaging; FF, fiber fraction; NAcc, nucleus accumbens

TABLE 1

Demographic data, monetary reward discounting, and eating and reward sensitivity behavioral domain summed *z* scores for participants with obesity and participants with normal weight

	People with obesity (*n* = 25)	**People with normal weight (*n* = 21)**	***p* value**
Age (y)	31.6 (6.4)	28 (5.2)	0.049 *
Sex (male/female)	4/21	5/16	0.55
Race/ethnicity	12 Black/13 White	2 Black/19 White (1 Hispanic)	0.012 *
Education level (y)	15.1 (1.8)	16.3 (1.6)	0.04 *
BMI (kg/m^2)	40 (5.0)	22 (2.2)	<0.001 ***
Body fat percentage (%)	48.8 (4.1)	32.6 (5.8)	<0.001 ***
Probabilistic reward discounting (AUC)	0.21 (0.06)	0.19 (0.11)	0.61
Delayed reward discounting (AUC)	0.52 (0.12)	0.53 (0.26)	0.99
Eating related to emotion summed *z* score	1.12 (2.57)	−1.5 (1.77)	<0.001 ***
Eating related to reward sensitivity summed *z* score	1.34 (1.68)	−1.78 (1.74)	<0.001 ***
Non-food reward sensitivity summed *z* score	−0.79 (2.1)	0.9 (1.9)	0.03 *
Sensitivity to punishment summed *z* score	0.51 (1.66)	−0.87 (2.89)	0.022 *

Independent Student *t* test, Mann-Whitney *U* test, or Pearson χ^2 tests were used as appropriate. Means (SD) or frequencies are reported.

Abbreviation: AUC, area under the curve.

* $p \leq 0.05$

*** $p \leq 0.001$.

TABLE 2

Basal ganglia volumes and DBSI metrics In people-with-obesity and people-with-normal-weight groups

	People with obesity (n = 25)	People with normal weight (n = 21)	p value
Caudate			
Volume (mm^3)	3,590 (268)	3,766 (438)	0.006***
DBSI fiber fraction	0.31 (0.02)	0.31 (0.02)	0.8
DBSI nonrestricted fraction	0.42 (0.03)	0.40 (0.03)	0.01***
DBSI restricted fraction	0.083 (0.01)	0.076 (0.01)	0.17
Globus pallidus			
Volume (mm^3)	1,774 (114)	1,791 (149)	0.06
DBSI fiber fraction	0.59 (0.06)	0.57 (0.05)	0.11
DBSI nonrestricted fraction	0.17 (0.04)	0.2 (0.05)	0.12
DBSI restricted fraction	0.170 (0.03)	0.155 (0.03)	0.33
Nucleus accumbens			
Volume (mm^3)	518 (68)	501 (88)	0.048*
DBSI fiber fraction	0.39 (0.06)	0.47 (0.05)	<0.0001***
DBSI nonrestricted fraction	0.44 (0.05)	0.39 (0.06)	<0.0001***
DBSI restricted fraction	0.095 (0.02)	0.092 (0.02)	0.81
Putamen			
Volume (mm^3)	4,994 (405)	5,056 (351)	0.22
DBSI fiber fraction	0.36 (0.02)	0.39 (0.02)	0.0005***
DBSI nonrestricted fraction	0.45 (0.03)	0.45 (0.03)	0.71
DBSI restricted fraction	0.127 (0.02)	0.108 (0.01)	0.004***

Average volumes and average DBSI metrics were compared between people with obesity and people with normal weight using a multiple linear regression model with age, sex, race, and level of education as covariates. Volumes were normalized for total intracranial volume. Means (SD) are reported.

Abbreviation: DBSI, diffusion basis spectrum imaging.

*$p \leq 0.05$

***$p \leq 0.01$.